Journal of Materials Chemistry C

Accepted Manuscript

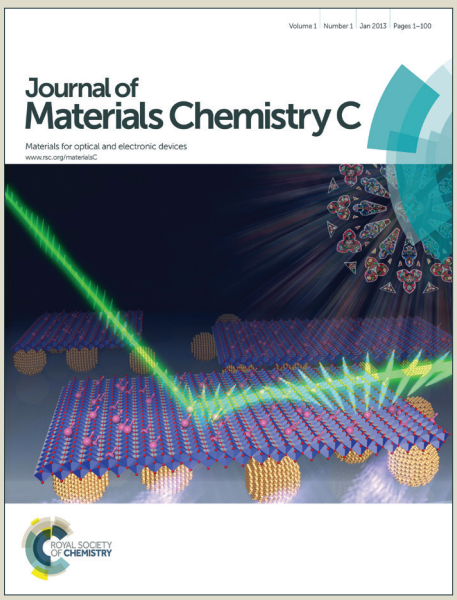

ROYAL SOCIETY OF CHEMISTRY

www.rsc.org/materialsC

Facile access to B-doped solid-state fluorescent carbon dots toward light emitting devices and cell imaging agent

Chen Shen, Jing Wang, Yi Cao, Yun Lu*

Department of Polymer Science and Engineering, State Key Laboratory of Coordination Chemistry, Key Laboratory of High Performance Polymer Materials and Technology (Nanjing University), Ministry of Education, School of Chemistry and Chemical Engineering, Nanjing University, Nanjing 210093, PR China

* Prof. Dr. Yun Lu, Corresponding author

Department of Polymer Science and Engineering, State Key Lab Coordination Chemistry, School of Chemistry and Chemical Engineering, Nanjing University, Nanjing 210093, China

E-mail: yunlu@nju.edu.cn

Keywords: B-doped carbon nanodots, solid-state fluorescent, bioimaging, light emitting devices

Abstract A green and facile hydrothermal approach for carbonizing boric acid and ethylenediamine into B-doped carbon dots (CDs) has been proposed, providing a new way to synthesize functional carbon dots in a large scale. The obtained B-doped CDs

exhibit favorable aqueous solubility and strong fluorescence in both aqueous and solid states. Especially, the unique solid-state fluorescence properties of the B-doped CDs inspire new thoughts for other applications, accordingly a yellowish-green light emitting diode with the as-obtained CDs as light converters is demonstrated. Meanwhile, the as-prepared CDs also display intensely low toxicity and excellent multicolour fluorescence imaging ability in live cell.

1. Introduction

Carbon dots (CDs) is a family member of carbon-based nanomaterials first proposed and isolated in 2004.[1] In recent years, CDs are inspiring intensive research interests owing to their high aqueous solubility, chemical inertness, low toxicity, facile functionalization and photo-bleaching resistance,[2-6] which make them a new generation luminescent materials superior to conventionally used fluorescent organic dyes and inorganic quantum dots. To date, there are mainly two types of the synthesis methods for CDs: top-down routes and bottom-up routes.[7] Top-down methods include arc-discharge, laser ablation, electrochemical oxidation, etc.,[1, 8, 9] where CDs are formed or "broken off" from larger carbon structures, such as graphite. Bottom-up methods involve combustion/thermal process, supported synthesis, microwave technique, etc.,[10-15] during which CDs are mainly prepared from molecular precursors. As a new kind of novel canbon functional materials, CDs are standing out and showing their potential applications in such fields as bioimaging, photocatalysis, optoelectronic devices, drug and gene delivery, chemical sensors and biosensors.[16-26]

However, several drawbacks for carbon dots should not be ignored. First, the quantum yield (QY) of CDs is much lower than that of the conventional semiconductor quantum dots.[7] Second, CDs can only exert good fluorescence in their dispersed solvents rather than in their dry and aggregated states due to the strong fluorescence quenching. And thirdly, the preparation process for functional CDs usually is multistep, with the use of organic reagents simultaneously. According to the above problems, various positive solutions have been put forward. For instance, the chemical doping with heteroatoms and introducing the organic amine passivants to tune the intrinsic properties of carbon nanomaterials have been reported successively,[27, 28] since the heteroatoms such as O, N, S, etc. could provide the density of states or emissive trap states for photoexcited electrons to modify the band-gap energy, thus offering functionalized CDs more optimized properties.[29-31] Meanwhile, some new-type heteroatoms, for example Al atoms, could highly improve the QY of CDs by doping the electron-deficient Al^{3+} ions in CDs, thus making as-prepared CDs a chemosensor with highly sensitive and selective response to Ga^{3+} ions in a wide concentration range.[32] However even so, few papers have been published that deal with the promotion of new optical properties for CDs by doping of different heteroatoms.[33-36] In addition, the solid-state luminescent application for heteroatom-doped CDs remains inchoate,[37-39] and need to be further explored. Therefore, it is an interesting project to develop CDs nanomaterials with high quantum yield, novel properties and promising applications through doping different heteroatoms in a green and simple way.

In this research, a green and facile strategy was developed for the hydrothermal synthesis of the boron-doped CDs with solid-state fluorescence properties by selecting boric acid and ethylenediamine as boron and carbon sources. The effects of the chemical compositions of the materials, especially the introduction of boron atoms, on photoluminescence behaviors of the as-prepared CDs were investigated systematically. On this basis, the unique properties for the B-doped CDs such as exceptional solid-state fluorescent feature and excellent biocompatibility were studied and applied in LED convertor material and live cell imaging reagent.

2. Experimental section

2.1 Materials

Boric acid (BA), ethylenediamine (EDA), acridine orange (AO), ethidium bromide (EB), and the other chemicals were analytically pure and used as received without further purification. Phosphate buffered saline (PBS) was purchased from Keygen Biotech Ltd. Doubly deionized water (DI, 18.2 MΩ·cm at 25 °C) prepared by a Milli-Q (MQ) water system was used throughout all experiments.

2.2 Preparation of carbon nanodots

BA was dissolved in the mixture solvent of DI water and ethylenediamine. Then the solution was transferred to a poly (p-phenylene) autoclave and heated at 260 °C for 12 hours. After the reaction, the reactor was cooled to room temperature naturally. The obtained dark brown solution was centrifuged at a high speed (15000 rad/min) for 15 min to remove the less-photoluminescent deposit. The upper brown solution exhibited

strong green luminescence under excitation at 365 nm UV light. The pure luminescent carbon dots were obtained by freeze dried and had a yield of about 50%.

2.3 Preparation of LED

A UV-LED chip with the peak wavelength centered at 430 nm was attached on the bottom of the LED base. The two leads on LED were prepared to connect to the power supply. Afterward, the thermo-curable resin was mixed with the as-prepared CDs powders (CDs/resin=1/10 wt/wt) and put in a vacuum chamber to remove the bubbles. The mixtures were coated on the LED chip and thermally cured at 150°C for 1 h.

2.4 *Cellular toxicity test and cellular imaging*

In toxicity test, acute myeloblastic leukemia cells (HL-60) in the exponential growth phase were washed by PBS twice. After digesting by 0.25% trypsin solution for 2 min, cells were suspended by PBS and washed twice. Then whole culture medium was added and cells suspension was transferred to 96-well plate with 200 μL in each well. In control group, 20 μL PBS was added to each well. In experimental group, 20 μL as-obtained CDs solution with different concentrations was added to each well. Cells were then cultured at 37 °C under 5% CO_2 in standard incubator for 12 hours, 24 hours and 48 hours, respectively. Then combined EB/AO staining was executed for cell state examination. 10 μL EB/AO (100 $\mu g \cdot mL^{-1}$) was added to each well. The resulting fluorescence images of the cells were monitored by the Leica DMIRE2

microscope fluorescence analyzing system. Cell viability data was captured by Image-Pro Plus (IPP) program.

Hela cells were cultured and propagated in a cover-glass-bottom dish in DMEM cell culture medium (Gibco) with 10% fetal bovine serum and 100 mg•L^{-1} penicillin and 100 mg•L^{-1} streptomycin at 37 °C under 5% CO_2 in standard incubator. After 12 hours incubation, fresh culture medium with the synthetic CDs (The final CDs' concentration is about 200 μg•mL^{-1}) was added to the cell culture dishes. Then, the cells were washed with PBS for three times to remove the excess CDs. Immediately after the incubation and washing steps, the images observation were taken by a confocal laser scanning microscope. The confocal analysis was performed on a ZEISS LSM710 laser scan confocal microscope.

2.5 Characterization methods

The morphologies of the samples were observed by scanning transmission electron microscopy (TEM, JEOL 2000FX). In each TEM measurements, one drop of diluted sample was placed on a copper grid covered with a nitrocellulose membrane and air dried before examination. The DLS (Dynamic light scattering) measurements were performed by using a Brookhaven BI9000AT system (Brookhaven Instruments Corporation) with a wavelength of 633.0 nm and a detection angle of 90° at 25 °C. Fourier-transform infrared spectra (FTIR) of samples in solid state (KBr matrix) were measured with a Bruker VECTOR22 spectrometer with 4 cm^{-1} resolution. The elemental analysis was carried on the equipment of Elementar Vario MICRO analyzer (Heraeus, Germany) under a test temperature of 950 °C. X-ray photoelectron

spectroscopy (XPS, ESCALB MK-II, VG Co., England) measurement was performed under a base pressure of 1×10^{-9} Torr using monochromatic Mg-K_α X-rays at h_v=1253.6 eV. The UV-vis spectra were recorded on Perkin Elmer Lambda 35 instrument with 1 nm resolution. The emission spectra were measured on FluoroMax Spectrofluorometer (HORIBA Jobin Yvon, France) with 1 nm resolution. The phase structures were examined by powder X-ray diffraction (XRD) (on a Shimadzu XD-3A instrument with Cu-Kα radiation (λ=1.5418Å) at room temperature. The zeta potential was determined by zeta potential analyzer (Malvern Zetasizer 3000HSA). The brightness and working voltage of the LED were examined by Keithley 2400/2000 and ST-86LA-3.

The quantum yield (Φ) of the CDs was calculated with the following equation. Quinine sulfate dissolved in 0.1 M H_2SO_4 (literature quantum yield 54% at 360 nm) was chosen as a standard. Where, Φ is the quantum yield, I is the measured integrated emission intensity, n is the refractive index, and A is the optical density. The subscript R refers to the Quinine sulfate. In the typical experiment, the quantum yield was measured at the excitation and emission wavelengths of 360 nm and 440 nm respectively.

$$\Phi = \Phi_R \times \frac{I}{I_R} \times \frac{A_R}{A} \times \frac{n^2}{n_R^2}$$

The quantum yield of the CDs in solid state was calculated with the following equation. Where, Φ_R is the quantum yield, I is the measured integrated intensity of the light source and I_R is the measured integrated emission intensity of the CDs.

$$\Phi_R = \frac{I_R}{I}$$

3. Results and Discussion

As starting materials, boric acid and ethylenediamine are widely accessiable and very cheap, and both obtain commendable solubilities in water or other organic solvents, so the preparation of carbon dots can be facilely applicable to a variety of solvent systems with prime dispersion. Besides, the electron-deficient boron atoms may bring new optical properties into the materials; ethylenediamine can provide the carbon and nitrogen atoms to form and dope the framework of the CDs. At the same time, the residual ethylenediamine after reaction can possess the effect of passivation agent, so as to leave out the surface modification step and improve the quantum efficiency of the product. Moreover, the as-prepared CDs have a relatively high productive yield about 50% much higher than that reported previously,[6, 7, 40, 41] which is very suitable for mass production.

TEM image (Fig.1A) shows that the as-prepared CDs are mostly spherical shapes in the diameter range of 1-6 nm with an average size of 2.84 nm (Fig.1B). Also, there are crystallinity region with a lattice parameter of 0.24 nm existing in the CDs (Fig.1A, inset), which may be attributed to the (100) facet of graphene.[42]

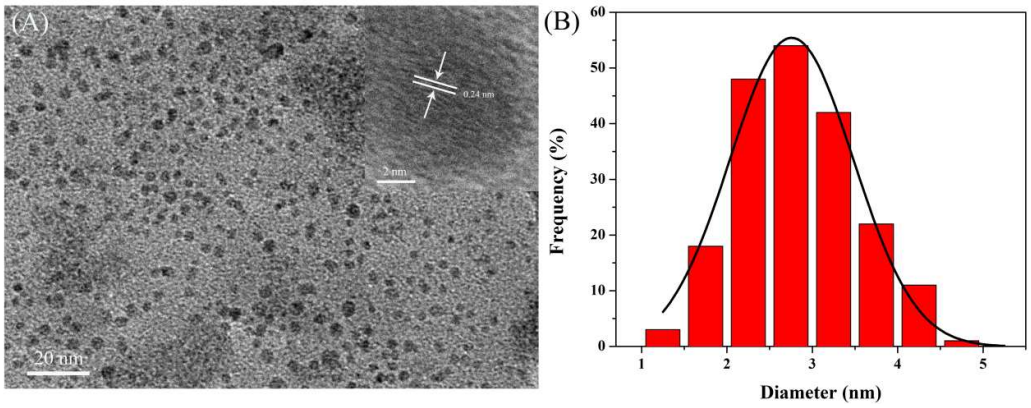

Fig.1 (A) TEM image and the high magnification image (inset) of the CDs. (B) The corresponding size distribution histogram.

The FTIR spectra of BA and the as-prepared CDs (Fig.2A) show that the characteristic absorptions of BA at 3226 and 1480 cm^{-1}, attributable to BO-H stretching and B-O asymmetric stretching vibrations respectively,[43] appear in the spectrum of the CDs but shift to 3120 and 1460 cm^{-1}, implying the presence of BA structure in the products and probable interaction between BA and the CDs. Beyond that, the peaks of some other functional groups can also be observed in the spectrum of the CDs. For instance, the broad peak at about 3430 cm^{-1} is attributed to the C-OH and C-NH stretching vibrations, indicating the presence of hydroxyl and amino groups. The peaks at 1645 cm^{-1} and 1394cm^{-1} are assigned to C=O stretching vibration and C-O stretching vibration respectively, manifesting the existence of COO^--functionalized surface of the CDs.[44, 45] These two oxygenated vibration peaks for the CDs are much higher than that for boric acid, suggesting that the hydrothermal carbonization can introduce abundant oxygenated groups, such as carbonyl and hydroxyl groups, through the thermal oxidation reactions.[46]

Different from BA, the obtained CDs shows a broad diffraction peak at 23.5º in its XRD pattern (Fig.2B), indicating that the interlayer spacing of the (002) diffraction peak is 0.39 nm. The spacing is larger than that of graphite (0.34 nm), probably thanks to the introduction of nitrogen-, boron- and oxygen-containing groups.[31]

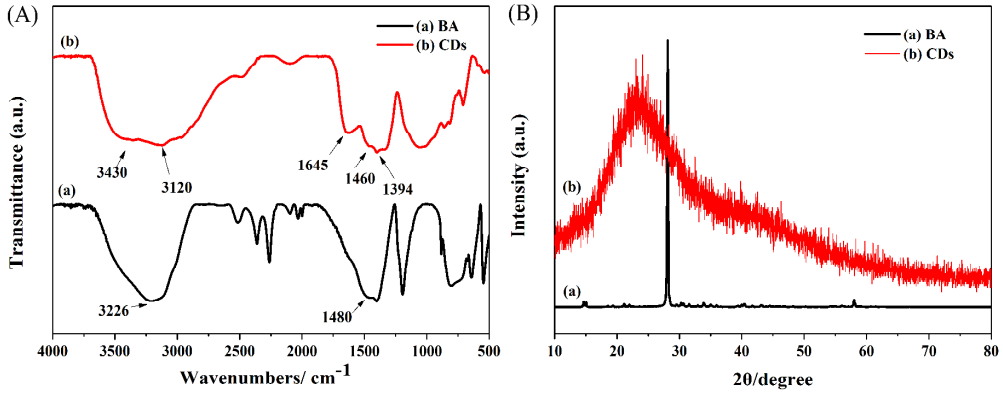

Fig. 2 (A) FT-IR spectra and (B) XRD patterns of (a) BA and (b) CDs.

The X-ray photoelectron spectroscopy (XPS) characterizations have also been carried out to explore the content and configuration of doped boron atoms in the CDs. The full range XPS analysis of the resultant CDs sample shown in Fig.3A clearly reveals the presence of boron (B), carbon (C), nitrogen (N) and oxygen (O) with atomic percentages of 6.5%, 63.15%, 11.52% and 18.47%, and the corresponding B1s, C1s, N1s and O1s peaks center at 190 eV, 284 eV, 400 eV and 532 eV respectively.[11, 43] The C1s core region spectrum (Fig. 3B) can be peak-differentiated to demonstrate several different types of carbon atoms including graphitic or aliphatic (C-C, 284.6 eV), oxygenated (C-O, 286.8 eV and O-C=O, 288eV), and nitrous (C-N, 286.0 eV).[11, 47] The high-resolution B1s spectrum of the synthetic CDs exhibits two peaks (Fig.3C). The peak at 192.0 eV is attributed to the B-O bonds, while the peak around 190.3 eV

is due to B-N bonds.[43] These XPS spectroscopic data agree well with the results of FTIR spectra, further confirming the presence of functional groups in the CDs and the coincident relationship between the reactants and products, which indicate that the surface functionalized B-doped CDs have been obtained successfully.

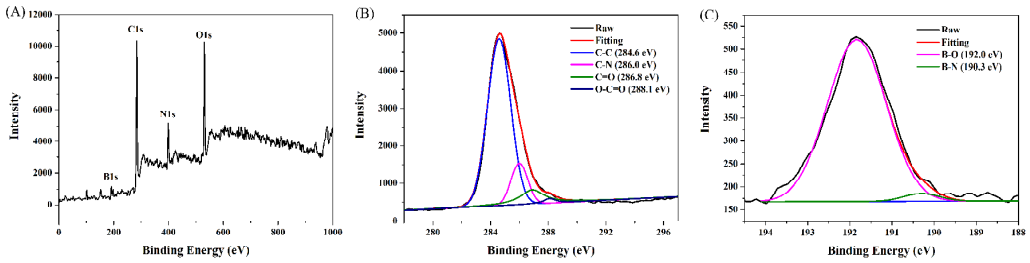

Fig.3 The XPS spectra of the CDs. (A) Overall spectrum, Core region spectra of (B) C1s and (C) B1s, after peak-differentiate-fitting.

Excellent optical properties are among the most fascinating features of CDs, and spur CD research and development in various applications. To explore further the optical properties of the B-doped CDs, their UV-Vis absorption and PL spectra are measured. The UV-Vis absorption spectrum of the CDs (Fig.4A) displays a quintessential absorption band located at 260 nm which belongs to the π-π* transition of the aromatic sp^2 domains, and should originate from the contribution of multiple-aromatic chromophores.[12, 48] The shoulder peak at 340 nm is ascribed to the n-π* transition of the C=O bond, confirming the existence of oxygen-containing groups in the CDs.[49] Also, because of the introduction of electron-deficient boron atoms, the B-doped CDs may obtain various surface traps with different energy levels,

which could bring in different transition modes and lead to the weak and asymmetric shoulder absorption peaks.[39]

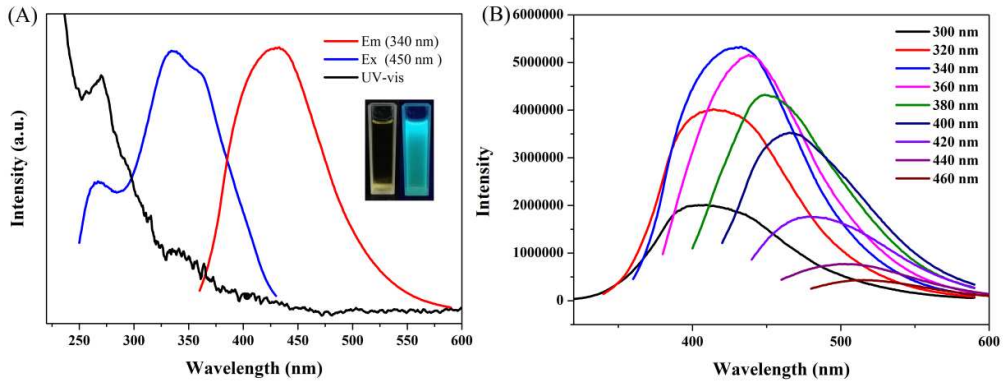

Fig. 4 (A) The UV-vis absorption, PL excitation and emission spectra of the CDs in aqueous solution. Insets show photographs of the CDs in aqueous solution under visible light (left) and UV light (right). (B) The excitation-dependent PL for the CDs.

As precursors, BA and EDA molecules themselves lack photoluminescent characteristics. However, the B-doped CDs possess strongest excitation and emission peaks at 340 nm and 430 nm respectively, and display a cyan color under a UV lamp (Fig. 4A and inset). As changing the excitation wavelength from 300 nm to 460 nm, the emission peaks of the as-prepared CDs clearly shift toward longer wavelengths with the increase of excitation wavelength (Fig.4B). Such tunable excitation-dependent PL behavior could be explained by multiple transition modes of the introduction of boron atoms,[39] and very useful in multicolor imaging applications. It is encouraging that the obtained CDs aqueous solution displayed a quantum yield of 22% using quinine sulfate as a reference, which reaches the comparatively high

standard of photoluminescent carbon-based materials, comparing to some carbon dots reported before.[28, 34, 37, 50]

Owning to the fact that the physical/chemical stability of CDs is of great significance to their practical applications, the effects of ion strength and UV exposure time on the PL stability of the B-doped CDs are also investigated. There is no prominent decrease in PL intensity or remarkable shifts in peak characteristics at different ion strengths, which is considerably larger than phosphate buffered saline (Fig.5A, B), showing the potential of the B-doped CDs at various physical salt concentrations in practical applications.[12] The photobleaching experiment was processed under the UV light of 12 W at the wavelength of 365 nm, and it is outstanding that no obvious photo-bleaching is found after 24 h of continuous UV excitation (Fig.5C, D), which should be a consequence of CDs' essential carbon structure and will be beneficial for the application of photo-luminescent device.[6]

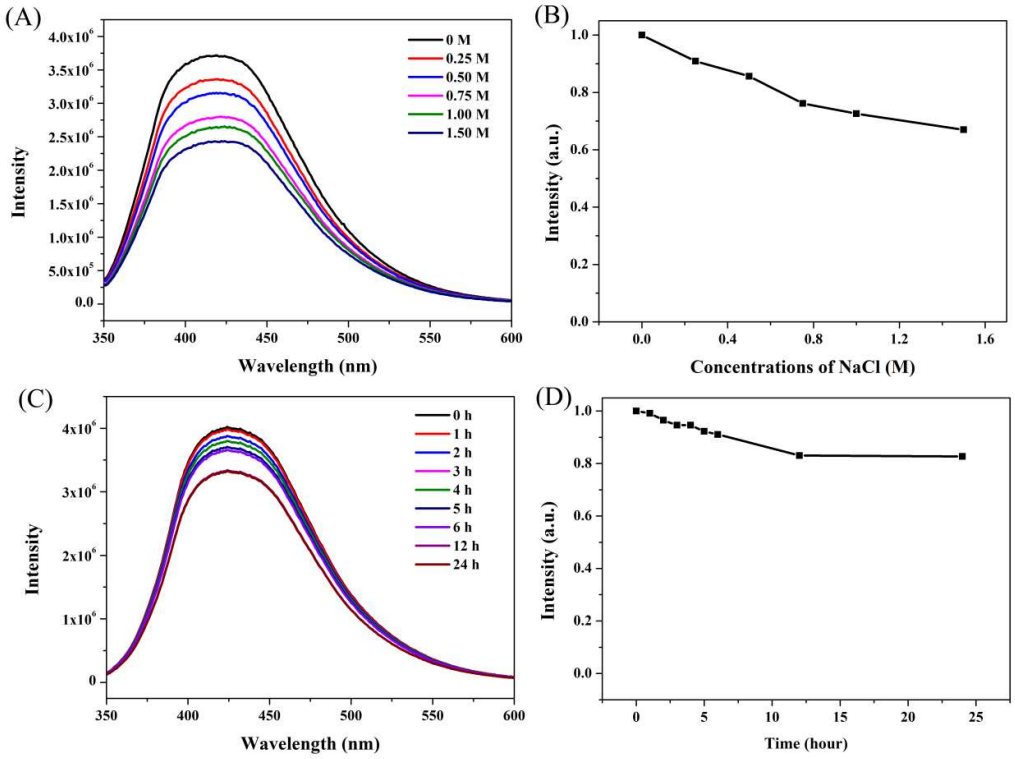

Fig.5 Stability of the CDs. (A and B) Effect of ionic strength on the CDs' fluorescence intensity (ionic strengths are controlled by various NaCl concentrations). (C and D) Dependence of fluorescence intensity on UV excitation time for the CDs in DI water

Aggregation-induced quenching phenomena usually occur with drying CDs into films or powders. In this research, one of the most encouraging results is that the B-doped CDs can also emit strong fluorescence in their solid state under UV lamp which can be observed by naked-eyes (Fig.6B, E). The quantum yield of the CDs in solid state is about 18%, which is nearly the same with the properity in aqueous state. It is found that the dry CDs powders are remarkably stable to disperse repeatedly into water without any aggregation, which is significant for preservation and transportation. Three sets of parallel experiments were carried out to further explore the origins for the special solid-state fluorescence properties of the as-prepared CDs.

Firstly, BA or EDA is required to undergo individually the hydrothermal reaction, and no solid-state fluorescent CDs is obtained either. For the former, BA is hard to form carbon dots due to its molecular structure without C element and also BA itself has no photoluminescent characteristics, as shown in Fig.6A, D. For the latter, although EDA can be carbonized into black carbon powders, no fluorescence is observed in their solid state (Fig.6C, F). The solid-state fluorescent CDs can only be obtained by the hydrothermal reaction of BA with EDA together, which can possibly be attributed to the introduction of B element. First, the electron-deficient B atom could restrain the intermolecular charge transfer among the CDs induced by the interaction between electron donors and acceptors, thus depressing the quenching caused by aggregations.[51] Second, the H-bonds interactions, which generates from the surface B-OH groups,[38] could make the agminated nanodots present a dispersive state similar to that in liquid media.[37] In addition, because of the presence of abundant negative electricity functional groups, the zeta potential of the CDs is about -25 mV, so the strong electrostatic repulsions among the carbon dots could prevent them from excessive aggregations.[39] For the foregoing resons, the PL properties of the B-doped CDs could be well persisted in the solid state.

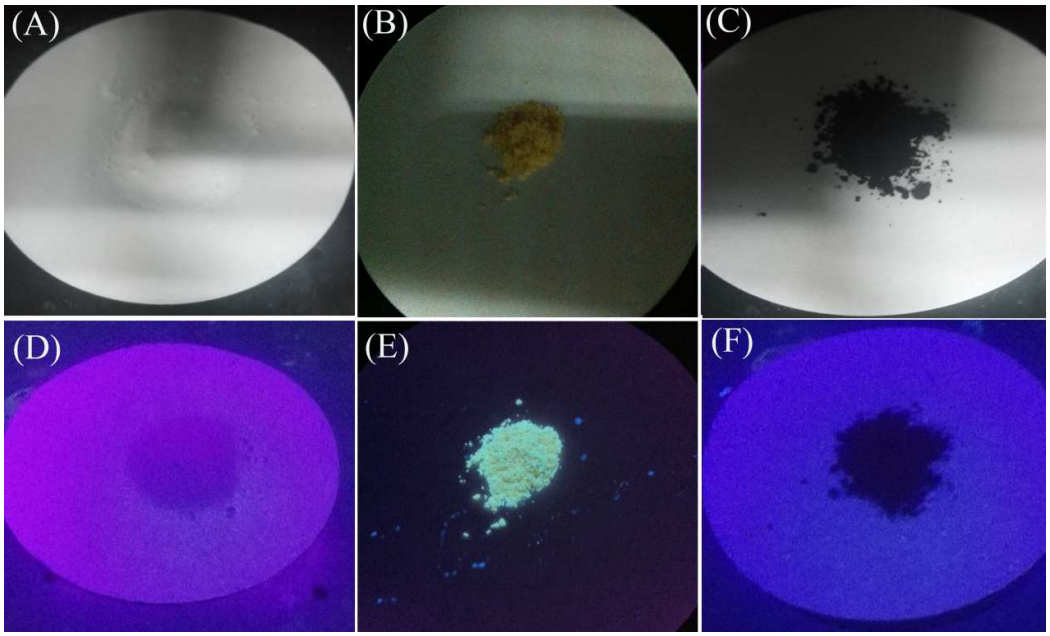

Fig.6 (A, D) boric acid, (B, E) B-doped carbon dots and (C, F) carbon dots derived from EDA under visible light (up) and under a 365 nm UV lamp (down).

By virtue of their strong fluorescence ability in solid state, the B-doped CDs could exhibit enormous practical applications in the lighting and display field. Here, a LED has been fabricated based on the resultant CDs, where the B-doped CDs/silicone mixtures are coated on a 430 nm UV chip and acted as light converters (Fig.7A).[50] The UV light emitted from the UV chip can be transformed into green-yellow light when passing through this CDs converter. For practical applications, the brightness of the LED is about 250 cd/cm^2 at the working voltage of 3.2 V and it is observed that the LED can illuminate the paper in the bright day (Fig.7B), indicating that the heavy metal-free CDs with stable optical properties are promising materials in the optoelectronic applications.

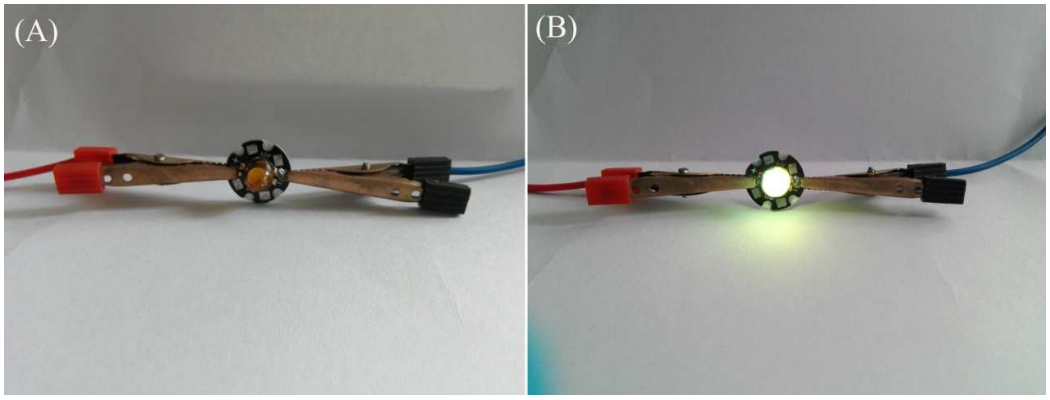

Fig.7 The photographs of the LED based on the B-doped CDs under (A) daylight and (B) operation condition.

As a new fluorescent probe, the B-doped CDs have been evaluated for its application in bioimaging and biolabeling in living cells. Fig. 8A makes it clear that the CDs exhibite extremely low cytotoxicity with cell viability at about 80%, even at a concentration of 100 μg/mL of the as-prepared CDs and at 48 h of exposure time. In addition, the bright-field optical images also validate that no morphological cell damage is observed upon incubation with the CDs, further demonstrating their low cytotoxicity. According to the observations by the confocal microscope, it is found that the labeled cells are brightly illuminated with multicolor images at different excitation wavelengths, due to the strong fluorescence emitting from the B-doped CDs (Fig.8C, D). The PL spots are found only in the cell membrane and cytoplasmic area of the cell but exceedingly weak at the central region corresponding to the nucleus, indicating that the CDs can easily penetrate into the cell but not enter the nuclei, in which the genetic disruption could not occur. The abovementioned results suggest that thanks to low toxicity, the as-prepared CDs enjoy great potential for use in biological applications, such as bioimaging, protein analysis by fluorescence

resonance energy transfer (FRET), cell tracking, isolation of biomolecules, and gene technology.

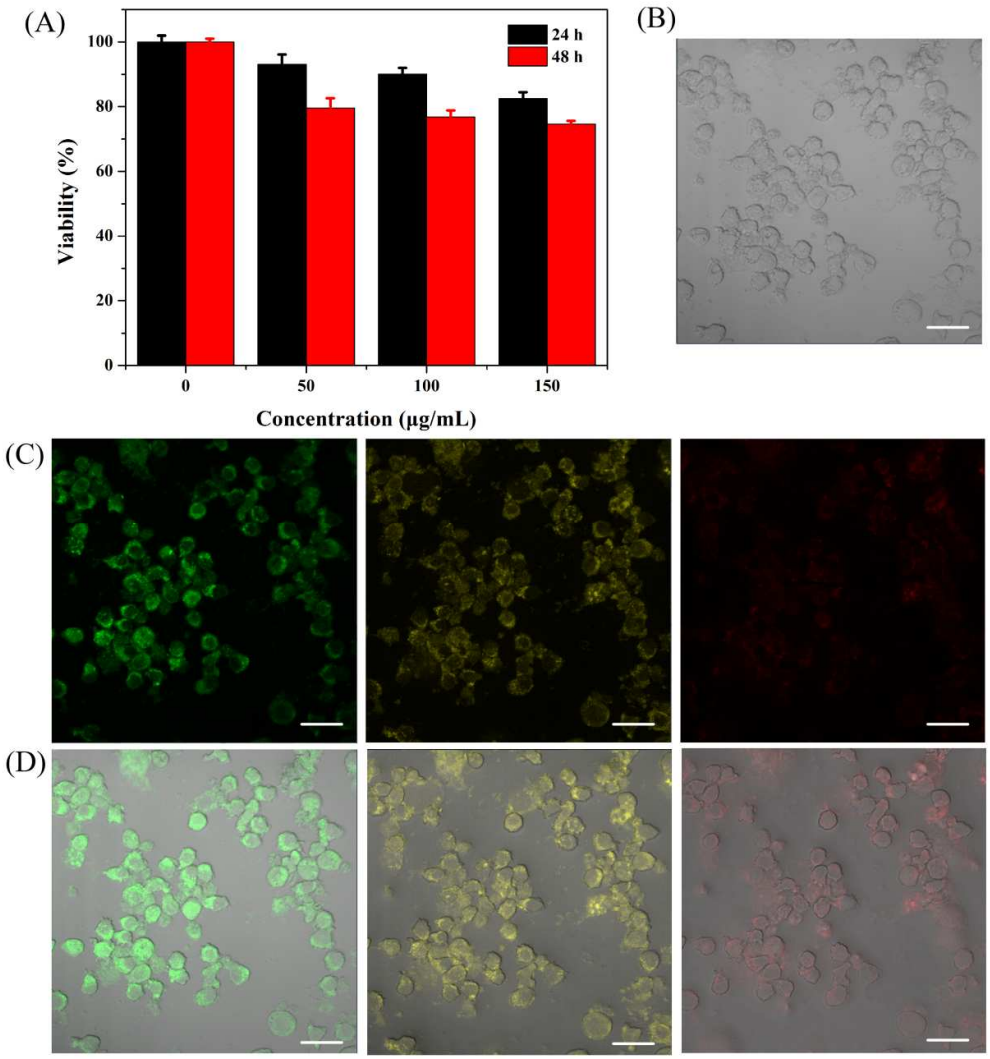

Fig. 8 Cellular toxicity and cellular imaging of the CDs. (A) Effect of the CDs on HL-60 cell viability. Washed cells imaged under (B) bright field, (C) confocal photoluminescent, and (D) overlap of corresponding bright field image and fluorescence image under the different excitation. (The scale bar is 5 μm)

4. Conclusion

The B-doped carbon dots have been conveniently prepared by means of a direct, facile and green hydrothermal method with a high yield about 50%, offering a possibility for their batch preparation. The obtained CDs possess uniform morphology, aboundant functional groups and B-doped structure, which endow them with the superior PL properties in both solid and aqueous states, and promising PL stabilities under high ion strength and long UV exposure time. The achieved quantum yield of the CDs is as high as 22%. Moreover, the CDs can be appropriately applied as LED convertor materials and cell-imaging agents because of the outstanding characteristics of solid-state PL properties and good biocompatibility.

Acknowledgement

This project was supported by the National Natural Science Foundation of China (No. 21174059, 21374046), Program for Changjiang Scholars and Innovative Research Team in University, Open Project of State Key Laboratory of Supermolecular Structure and Materials (SKLSSM2015015) and the Testing Foundation of Nanjing University.

References

1 X. Y. Xu, R. Ray, Y. L. Gu, H. J. Ploehn, L. Gearheart, K. Raker and W. A. Scrivens, *J. Am. Chem. Soc.*, 2004, **126**, 12736-12737.

2 L. Y. Zheng, Y. W. Chi, Y. Q. Dong, J. P. Lin and B. B. Wang, *J. Am. Chem. Soc.*, 2009, **131**, 4564-4565.

3 J. Shen, Y. Zhu, X. Yang and C. Li, *Chem. Commun.*, 2012, **48**, 3686-3699.

4 H. Li, Z. Kang, Y. Liu and S.-T. Lee, *J. Mater. Chem.*, 2012, **22**, 24230-24253.

5 Y. Li, Y. Hu, Y. Zhao, G. Shi, L. Deng, Y. Hou and L. Qu, *Adv. Mater.*, 2011, **23**, 776-780.

6 Y. P. Sun, B. Zhou, Y. Lin, W. Wang, K. A. S. Fernando, P. Pathak, M. J. Meziani, B. A. Harruff, X. Wang, H. F. Wang, P. J. G. Luo, H. Yang, M. E. Kose, B. Chen, L. M. Veca and S. Y. Xie, *J. Am. Chem. Soc.*, 2006, **128**, 7756-7757.

7 S. N. Baker and G. A. Baker, *Angew. Chem. Int. Ed.*, 2010, **49**, 6726-6744.

8 H. Gonçalves, P. A. S. Jorge, J. R. A. Fernandes and J. C. G. Esteves da Silva, *Sensor. Actuat. B-Chem.*, 2010, **145**, 702-707.

9 J. Lu, J. X. Yang, J. Z. Wang, A. Lim, S. Wang and K. P. Loh, *ACS Nano*, 2009, **3**, 2367-2375.

10 L. Tian, D. Ghosh, W. Chen, S. Pradhan, X. Chang and S. Chen, *Chem. Mater.*, 2009, **21**, 2803-2809.

11 S. Liu, J. Tian, L. Wang, Y. Zhang, X. Qin, Y. Luo, A. M. Asiri, A. O. Al-Youbi and X. Sun, *Adv. Mater.*, 2012, **24**, 2037-2041.

12 S. Zhu, Q. Meng, L. Wang, J. Zhang, Y. Song, H. Jin, K. Zhang, H. Sun, H. Wang and B. Yang, *Angew. Chem. Int. Ed.*, 2013, **52**, 3953-3957.

13 R. Liu, D. Wu, S. Liu, K. Koynov, W. Knoll and Q. Li, *Angew. Chem. Int. Ed.* , 2009, **48**, 4598-4601.

14 X. H. Wang, K. G. Qu, B. L. Xu, J. S. Ren and X. G. Qu, *J. Mater. Chem.*, 2011, **21**, 2445-2450.

15 S. Gao, Y. Chen, H. Fan, X. Wei, C. Hu, L. Wang and L. Qu, *Journal of Materials Chemistry A*, 2014, **2**, 6320-6325.

16 G. Wu, F. Zeng, C. Yu, S. Wu and W. Li, *J. Mater. Chem. B*, 2014, **2**, 8528-8537.

17 J. Xu, F. Zeng, H. Wu, C. Hu, C. Yu and S. Wu, *Small*, 2014, **10**, 3750-3760.

18 C. Yang, R. P. Thomsen, R. Ogaki, J. Kjems and B. M. Teo, *J. Mater. Chem. B*, 2015.

19 C. Shen, Y. Sun, J. Wang and Y. Lu, *Nanoscale*, 2014, **6**, 9139-9147.

20 H. Li, R. Liu, S. Lian, Y. Liu, H. Huang and Z. Kang, *Nanoscale*, 2013, **5**, 3289-3297.

21 H. Choi, S.-J. Ko, Y. Choi, P. Joo, T. Kim, B. R. Lee, J.-W. Jung, H. J. Choi, M. Cha, J.-R. Jeong, I.-W. Hwang, M. H. Song, B.-S. Kim and J. Y. Kim, *Nat. Photonics*, 2013, **7**, 732-738.

22 C. Liu, P. Zhang, X. Zhai, F. Tian, W. Li, J. Yang, Y. Liu, H. Wang, W. Wang and W. Liu, *Biomaterials*, 2012, **33**, 3604-3613.

23 M. Zheng, S. Liu, J. Li, D. Qu, H. Zhao, X. Guan, X. Hu, Z. Xie, X. Jing and Z. Sun, *Adv. Mater.*, 2014, **26**, 3554-3560.

24 C. Wang, Z. Xu, H. Cheng, H. Lin, M. G. Humphrey and C. Zhang, *Carbon*, 2015, **82**, 87-95.

25 C. Yu, X. Li, F. Zeng, F. Zheng and S. Wu, *Chem. Commun.*, 2013, **49**, 403-405.

26 Y. Guo, L. Zhang, S. Zhang, Y. Yang, X. Chen and M. Zhang, *Biosens. Bioelectron.*, 2015, **63**, 61-71.

27 S. Hu, R. Tian, Y. Dong, J. Yang, J. Liu and Q. Chang, *Nanoscale*, 2013, **5**, 11665-11671.

28 Q. Hu, M. C. Paau, Y. Zhang, X. Gong, L. Zhang, D. Lu, Y. Liu, Q. Liu, J. Yao and M. M. F. Choi, *RSC Adv.*, 2014, **4**, 18065-18073.

29 L. Tang, R. Ji, X. Li, K. S. Teng and S. P. Lau, *J. Mater. Chem. C*, 2013, **1**, 4908-4915.

30 L. Zhang and Z. Xia, *J. Phy. Chem. C*, 2011, **115**, 11170-11176.

31 D. Sun, R. Ban, P.-H. Zhang, G.-H. Wu, J.-R. Zhang and J.-J. Zhu, *Carbon*, 2013, **64**, 424-434.

32 H. Wang, Y. Wang, J. Guo, Y. Su, C. Sun, J. Zhao, H. Luo, X. Dai and G. Zou, *Rsc Advances*, 2015, **5**, 13036-13041.

33 L. Zhang, Z. Y. Zhang, R. P. Liang, Y. H. Li and J. D. Qiu, *Anal. Chem.*, 2014, **86**, 4423-4430.

34 X. Shan, L. Chai, J. Ma, Z. Qian, J. Chen and H. Feng, *The Analyst*, 2014, **139**, 2322-2325.

35 M. K. Barman, B. Jana, S. Bhattacharyya and A. Patra, *J. Phys. Chem. C*, 2014, **118**, 20034-20041.

36 S. Jahan, F. Mansoor, S. Naz, J. Lei and S. Kanwal, *Anal. Chem.*, 2013, **85**, 10232-10239.

37 Y. Deng, X. Chen, F. Wang, X. Zhang, D. Zhao and D. Shen, *Nanoscale*, 2014, **6**, 10388-10393.

38 M. Xu, G. He, Z. Li, F. He, F. Gao, Y. Su, L. Zhang, Z. Yang and Y. Zhang, *Nanoscale*, 2014, **6**, 10307-10315.

39 X. Li, S. Zhang, S. A. Kulinich, Y. Liu and H. Zeng, *Sci. Rep.*, 2014, **4**, 4976-4984.

40 X. Sun and Y. Li, *Angew. Chem., Int. Ed.*, 2004, **43**, 597-601.

41 S. Y. Lim, W. Shen and Z. Gao, *Chem. Soc. Rev.*, 2015, **44**, 362-381.

42 J. Peng, W. Gao, B. K. Gupta, Z. Liu, R. Romero-Aburto, L. Ge, L. Song, L. B. Alemany, X. Zhan, G. Gao, S. A. Vithayathil, B. A. Kaipparettu, A. A. Marti, T. Hayashi, J. J. Zhu and P. M. Ajayan, *Nano Lett.*, 2012, **12**, 844-849.

43 X. Liu, S. Ye, Y. Qiao, G. Dong, Q. Zhang and J. Qiu, *Chem. Commun.*, 2009, 4073-4075.

44 V. Gupta, N. Chaudhary, R. Srivastava, G. D. Sharma, R. Bhardwaj and S. Chand, *J. Am. Chem. Soc.*, 2011, **133**, 9960-9963.

45 Y. Dong, J. Shao, C. Chen, H. Li, R. Wang, Y. Chi, X. Lin and G. Chen, *Carbon*, 2012, **50**, 4738-4743.

46 M.-M. Titirici, R. J. White, C. Falco and M. Sevilla, *Energy Environ. Sci.*, 2012, **5**, 6796-6823.

47 L. Bao, Z. L. Zhang, Z. Q. Tian, L. Zhang, C. Liu, Y. Lin, B. Qi and D. W. Pang, *Adv. Mater.*, 2011, **23**, 5801-5806.

48 S. J. Yu, M. W. Kang, H. C. Chang, K. M. Chen and Y. C. Yu, *J. Am. Chem. Soc.*, 2005, **127**, 17604-17605.

49 Y. R. Chang, H. Y. Lee, K. Chen, C. C. Chang, D. S. Tsai, C. C. Fu, T. S. Lim, Y. K. Tzeng, C. Y. Fang, C. C. Han, H. C. Chang and W. Fann, *Nat. Nanotechnol.*, 2008, **3**, 284-288.

50 L.-H. Mao, W.-Q. Tang, Z.-Y. Deng, S.-S. Liu, C.-F. Wang and S. Chen, *Ind. Eng. Chem. Res.*, 2014, **53**, 6417-6425.

51 X. Li, Y. Liu, X. Song, H. Wang, H. Gu and H. Zeng, *Angewandte Chemie*, 2015, **54**, 1759-1764.